Phase Diagram of Poly(ethylene oxide) and Poly(propylene oxide) Triblock Copolymers in Aqueous Solutions

Run Jiang, Qinghua Jin, Baohui Li, and Datong Ding

College of Physics, Nankai University, Tianjin 300071, China

An-Chang Shi*

Department of Physics & Astronomy, McMaster University, Hamilton, Ontario L8S 4M1, Canada

Received March 31, 2006; Revised Manuscript Received June 29, 2006

ABSTRACT: The phase behavior of poly(ethylene oxide) (PEO) and poly(propylene oxide) (PPO) triblock copolymers in aqueous solutions is studied by using a self-consistent-field theory. The spectral method is extended to polymer models with internal degrees of freedom. Phase diagrams of PEO−PPO−PEO and PPO−PEO−PPO triblock copolymers in water are constructed in the concentration−temperature space. A variety of lyotropic liquid crystalline phases is found. The effects of temperature, copolymer concentration, the block (EO/PO) ratio and the chain architecture are investigated. Good agreements were found between experimental results and theory.

I. Introduction

Block copolymers have attracted considerable attention due to their ability to self-assemble into various ordered structures.[1,2] For diblock copolymer melts, these structures range from lamellae, hexagonal-packed cylinders, and body-centered cubic sphere phases to a complex bicontinuous gyroid phase. These structures can be controlled by varying the composition of the block copolymers or the degree of segregation between the blocks.[3]

When block copolymers are mixed with solvents which dissolve only one of the blocks, the molecules self-assemble into specific structures to avoid direct contact between the solvents and the blocks which are insoluble. This mechanism gives rise to a wide range of self-assembled structures, including micelles of various shapes and size, as well as a variety of lyotropic liquid crystalline phases. Recently, there is a growing interest in the phase behavior of block copolymers in selective solvents.[4−7] In contrast to the case of block copolymer melts, where mainly the blocks ratio controls the structure, for binary block copolymer−solvent systems the contribution of the selective solvents to the interfacial curvature plays an important role.

Amphiphilic copolymers constituted by three alternate blocks of poly(ethylene oxide) (PEO) and poly(propylene oxide) (PPO) have a wide range of applications such as emulsifiers, wetting agents, solubilizers, etc.[8] Two of the possible block sequences are available: triblock copolymers with a PEO−PPO−PEO sequence (trade name Pluronic) and those with a PPO−PEO−PPO sequence (trade name Pluronic-R). These copolymers are denoted by $(EO)_n(PO)_m(EO)_n$ (Pluronic) and $(PO)_m(EO)_n(PO)_m$ (Pluronic-R), where n and m represent the numbers of EO and PO units, respectively. Water is a good solvent for the PEO blocks and a relatively poor solvent for the PPO blocks. Consequently, in aqueous solutions, solubility of the segments is the main factor which determines the internal domain structure. A remarkable structural polymorphism has been observed in block copolymer systems in the presence of selective solvent by varying the copolymer concentration or temperature.[9] Structural parameters such as the block copolymer molecular weight and the block (EO/PO) ratio are important variables influencing the form of different phases.[10] Furthermore, the chain architecture (PEO−PPO−PEO sequence or PPO−PEO−PPO sequence) is also expected to influence the phase behavior of the copolymers.

The phase diagrams for PEO−PPO−PEO block copolymers in aqueous solutions have been examined using a self-consistent mean-field theory (SCMFT) by Noolandi, Shi, and Linse.[11] The decreased solubility of EO and PO segments upon increasing temperature was modeled by a two-state model in which the monomers of the chain may assume two interconverting forms characterized by different interaction energies. In particular, one monomer state (A) is assumed to be hydrophilic while the other monomer state (B) is assumed to be hydrophobic. The calculations by Noolandi and co-workers were carried out by employing continuum and lattice versions of the SCMFT. Both methods predicted the following sequence of stable phases with increasing copolymer concentration: disordered polymer-poor solution (L_1), ordered cubic phase (I_1), hexagonal phase (H_1), lamellar phase (L_α), reverse hexagonal phase (H_2), reverse ordered cubic phase (I_2), and disordered polymer-rich solution (L_2). This phase transition sequence is in qualitative agreement with the corresponding experimental phase diagrams. It should be noticed that the calculations by Noolandi et al. were carried out in real space with the spherical unit cell approximation. As a consequence, they were unable to account for the gyroid phase. It is therefore desirable to carry out more accurate studies using the state-of-the-art reciprocal space method.

Another motivation of the current study is that, although a large number of papers on the phase behavior of PEO−PPO−PEO triblock copolymers have been published in the past few years,[9−12] only a few studies have been published on the triblock copolymers with the molecular architecture PPO−PEO−PPO (Pluronic-R).[13,14] In this paper we examine theoretically the phase behavior of both PEO−PPO−PEO and PPO−PEO−PPO copolymers in aqueous solutions. To do so, we extend the reciprocal space method to polymer models with internal degrees of freedom, and apply it to the two-state model for the PEO/PPO copolymers. This technique provides the most ac-

* To whom correspondence should be addressed. Telephone: (905) 525-9140 ext. 24060. Fax: (905) 521-2773. E-mail: shi@mcmaster.ca.

10.1021/ma060729d CCC: $33.50
Published on Web 07/29/2006

curate method to find numeric solutions of the SCMFT equations and, more importantly, it enables us to include the gyroid phase, which was lacking in earlier theoretical studies, in the calculations. As a consequence of this development, theoretical phase diagrams of both PEO−PPO−PEO and PPO−PEO−PPO triblock copolymers in aqueous solutions are constructed and presented in this paper.

The paper is organized as follows. Section II contains a description of the theoretical model employed in our study. Section III presents the calculated binary concentration−temperature phase diagrams for two PEO−PPO−PEO block copolymers and two PPO−PEO−PPO block copolymers. These systems were selected to emphasize the effects of different factors, such as temperature, copolymer concentration, the block (EO/PO) ratio and the chain architecture, on the phase behaviors. The density profiles for P84 are studied in detail for two different temperatures and three different morphologies (H_1, L_α, and H_2). Section IV contains conclusions while some mathematical details are given in the Appendix.

II. Theoretical Model

The theoretical framework used in the current study is based on an earlier theoretical model developed by Noolandi, Shi and Linse[11] for describing multicomponent mixtures of copolymers with internal degrees of freedom. The polymer chains are modeled as flexible Gaussian chains described by $\mathbf{R}_{pj}(t)$, where $\mathbf{R}_{pj}(t)$ denotes the position of the tth segment of the jth chain of type p. The degrees of polymerization of the p-chains are denoted by Z_p. The probability distribution $P_p(\{\mathbf{R}_{pj}(t)\})$ for a given block has the standard Wiener form

$$P_p(\{\mathbf{R}_p(t)\}) = A \exp\left\{-\frac{3}{2b_p^2}\int_0^{Z_p} \mathrm{d}t\left(\frac{d\mathrm{R}_p(t)}{\mathrm{d}t}\right)^2\right\} \qquad (1)$$

where A is a normalization constant and b_p is the Kuhn length of the p-chain. The partition function for a multicomponent polymer blend, including solvents, is given as a functional integral over all space curves representing the polymer chains.[15]

The Karlström model[16] was employed to describe the decreased solubility of the EO- and PO-containing polymers in water with increasing temperature. For the specific case of interests here, the EO and PO segments are assumed to have two conformational states, one being more polar with a lower energy and a lower statistical weight and one being less polar, having a higher energy and higher statistical weight. The population of the polar state is favored at lower temperatures, whereas the nonpolar state is favored at higher temperatures. This approach has previously led to a successful description of the inverse temperature behavior of different systems.[16−22] The internal states of the polymer chains are described by an index $\alpha_{pj}(t)$, which denotes the internal states of the tth segment of the jth chain of type p. The internal degree of freedom are populated according to a Boltzmann distribution independent of the spatial arrangement of the polymer chains such that the internal state distribution function $p_p(\{\alpha_{pj}(t)\})$ has the form,

$$p_p(\{\alpha_p(t)\}) = g_{p,\alpha p}(t)\mathrm{e}^{-\beta E_{p,\alpha_p(t)}} \qquad (2)$$

where $\beta = 1/k_BT$, $g_{p,\alpha p}(t)$ is the degeneracy of the $\alpha_p(t)$-states, and $E_{p,\alpha p}(t)$ is the energy of that state. These parameters have been determined from an independent analysis of the experimental data for the corresponding homopolymers[11] and are reproduced in Table 1.

Table 1. Internal State Parameters (E_{AB} and g_{AB})and Flory−Huggins Interaction Parameters($\chi_{BB'}$) of the Theoretical Model (Energy in kJ mol^{-1})

species	state	state no.	E_{AB}	g_{AB}
water		1	0	1
EO	polar	2	0[a]	1[a]
	nonpolar	3	5.086[a]	8[a]
PO	polar	4	0[b]	1[b]
	nonpolar	5	11.5[b]	60[b]

	$kT\chi_{BB'}$			
state no.	2	3	4	5
1	0.6508[a]	5.568[a]	1.7[a]	8.5[b]
2		1.266[a]	1.8[c]	3.0[c]
3			0.5[c]	−2.0[c]
4				1.4[b]

[a] From the fit to the experimental data of the binary PEO/water phase diagram.[16,23] [b] From the fit to the experimental data of the binary PPO/water phase diagram.[18] [c] From the fit to the experimental data of the ternary PEO/PPO/water phase diagram.[17]

The theory is formulated using a canonical ensemble. For a fixed volume V, we assume that the number of polymer chains of type p is n_p, and the number of solvent molecules is n_s. For a given chain configuration $\{\mathbf{R}_{pj}(t)\}$, the concentrations of solvent molecule and different monomers at a given spatial position $\mathbf{r}$ and state α are

$$\hat{\phi}_s(\mathbf{r}) = \frac{1}{\rho_{0s}}\sum_{i=1}^{n_s}\delta(\mathbf{r} - \mathbf{R}_{si}) \qquad (3)$$

$$\hat{\phi}_{p\alpha}(\mathbf{r}) = \frac{1}{\rho_{0p}}\sum_{j=1}^{n_p}\int_0^{Z_p}\mathrm{d}t\,\delta(\mathbf{r} - \mathbf{R}_{pj}(t))\delta_{\alpha,\alpha_{pj}(t)} \qquad (4)$$

where ρ_{0s} and ρ_{0p} represent the density of solvent molecules and polymer monomers, respectively.

The interactions between the monomers and solvents are modeled by short-range contact potentials and have the standard Flory−Huggins form

$$\frac{W(\{\hat{\phi}\})}{k_BT} = \int \mathrm{d}\mathbf{r}\left\{\sum_{P\alpha}\chi_{s,P\alpha}\rho_0\hat{\phi}_s(\mathbf{r})\hat{\phi}_{P\alpha}(\mathbf{r}) + \frac{1}{2}\sum_{P\alpha,P'\alpha'}\chi_{P\alpha,P'\alpha'}\rho_0\hat{\phi}_{P\alpha}(\mathbf{r})\hat{\phi}_{P'\alpha'}(\mathbf{r})\right\} \qquad (5)$$

where ρ_0 is a reference density, and $\chi_{s,P\alpha}$ are the Flory−Huggins parameters between solvent molecule and monomers and $\chi_{P\alpha,P'\alpha'}$ are the Flory−Huggins parameters between different monomers. The Flory−Huggins parameters of the various polymer components in their different internal states have been determined from the experimental data of homopolymers in solutions (Table 1).

Because exact evaluation of the partition function is in general not possible, a variety of approximate methods have been developed. The most fruitful method is the mean-field approximation, which amount to evaluating the functional integral using a saddle-point technique.[11] The result of this procedure is that the interacting many-chain problem is reduced to that of an independent chain subject to an external (mean) field, which in turn is created by all the polymer chains. The fundamental quantity to be evaluated is the propagators $Q_p(\mathbf{r},t|\mathbf{r}')$, which represents the distribution function of a polymer p with monomer t at r, given that monomer 0 is at $\mathbf{r}'$, in the presence

of an external field $\omega_p(\mathbf{r})$. It is straightforward to show that the propagators satisfy a modified diffusion equation.[24]

To include the effect of the internal states, as shown by Noolandi, Shi and Linse,[11] the internal states can be considered as embedded in an external field determined by the spatial arrangement of the molecules. The resulting effective potential is given by

$$\omega_p^{eff}(\mathbf{r}) = -\ln\left\{\sum_\alpha g_{p\alpha} \exp[-\beta E_{p\alpha} - \omega_{p\alpha}(\mathbf{r})]\right\} \quad (6)$$

which represents the statistically weighted thermal distribution of the internal states in an external mean fields, $\omega_{p\alpha}(\mathbf{r})$. The modified diffusion equation for $Q_p(\mathbf{r},t|\mathbf{r}')$ then has the standard form,

$$\frac{\partial}{\partial t}Q_p(\mathbf{r},t|\mathbf{r}') = \frac{b_p^{\,2}}{6}\nabla^2 Q_p(\mathbf{r},t|\mathbf{r}') - \omega_p^{\text{eff}}(\mathbf{r})Q_p(\mathbf{r},t|\mathbf{r}') \quad (7)$$

with the initial conditions, $Q_p(\mathbf{r},0|\mathbf{r}') = \delta(\mathbf{r}-\mathbf{r}')$. For simplicity we will assume that all the blocks have the same Kuhn length $b_p = b$.

We now use PEO−PPO−PEO (A_1−B−A_2) triblock copolymers in selective solvents as an example to formulate the theory. Extension to the case of PPO−PEO−PPO (B_1−A−B_2) triblock copolymers is straightforward. For a system of A_1−B−A_2 triblock copolymers in selective solvents, the partition function of a single chain subject to the effective potential $\omega_p^{\text{eff}}(\mathbf{r})$ is given by

$$Q_c = \frac{1}{V} \int d\mathbf{r}_1\, d\mathbf{r}_2\, d\mathbf{r}_3\, d\mathbf{r}_4\; Q_{A1}(\mathbf{r}_1,N_{A1}|\mathbf{r}_2)Q_B(\mathbf{r}_2,N_B|\mathbf{r}_3)Q_{A2}(\mathbf{r}_3,N_{A2}|\mathbf{r}_4) \quad (8)$$

where V is the volume of the system and the propagators $Q_p(\mathbf{r},t|\mathbf{r}')$ individually satisfy the modified diffusion equation (eq 7). The free energy of the system, F, has the form,

$$\frac{F}{k_B T\rho_0 V} = \frac{1}{V}\int d\mathbf{r}\left\{\sum_{P\alpha}\chi_{s,P\alpha}\phi_s(r)\phi_{P\alpha}(\mathbf{r}) + \frac{1}{2}\sum_{P\alpha,P'\alpha'}\chi_{P\alpha,P'\alpha'}\phi_{P\alpha}(\mathbf{r})\phi_{P'\alpha'}(\mathbf{r}) - \sum_{P\alpha}\frac{\rho_{0P}}{\rho_0}\omega_{P\alpha}(\mathbf{r})\phi_{P\alpha}(\mathbf{r}) - \omega_s(\mathbf{r})\phi_s(\mathbf{r}) - \frac{\eta(\mathbf{r})}{\rho_0}\left(1-\phi_s(\mathbf{r})-\sum_{P\alpha}\phi_{P\alpha}(\mathbf{r})\right)\right\} + \bar{\phi}_s \ln\left(\frac{\bar{\phi}_s}{Q_s}\right) + \frac{\bar{\phi}_c}{\tau_c}\ln\left(\frac{\bar{\phi}_c}{Q_c}\right) \quad (9)$$

where we have assumed that the solvent density, ρ_{0s}, is equal to the reference density$\rho_0$and the single particle partition function of the solvents Q_s is simply given by[15]

$$Q_s = \frac{1}{V}\int d\mathbf{r}\; e^{-\omega_s(\mathbf{r})} \quad (10)$$

which is a functional of the fields $\omega_s(\mathbf{r})$. The overall volume fraction of the solvent molecules and the copolymer is denoted by $\bar{\phi}_s$ and $\bar{\phi}_c$, respectively. The effective degrees of polymerization τ_p are $\tau_p = (\rho_{0s}/\rho_{0p})Z_p$, and $\tau_c = \tau_{A1} + \tau_B + \tau_{A2}$ for the A_1−B−A_2 triblock copolymers. The Lagrangian multiplier $\eta(r)$ is chosen to ensure the incompressibility condition. Minimizing the free energy given by eq 9 with respect to $\eta(\mathbf{r})$, $\phi_s(\mathbf{r})$, $\phi_{p\alpha}(\mathbf{r})$, $\omega_s(\mathbf{r})$, and $\omega_{p\alpha}(\mathbf{r})$ yields a set of self-consistent mean-field equations,

$$1 - \phi_s(\mathbf{r}) - \sum_{P\alpha}\phi_{P\alpha}(\mathbf{r}) = 0 \quad (11)$$

$$\omega_s(\mathbf{r}) = \sum_{P\alpha}\chi_{s,P\alpha}\phi_{P\alpha}(\mathbf{r}) + \frac{\eta(\mathbf{r})}{\rho_0} \quad (12)$$

$$\omega_{P\alpha}(\mathbf{r}) = \frac{\rho_0}{\rho_{0P}}\chi_{s,P\alpha}\phi_s(\mathbf{r}) + \frac{\rho_0}{\rho_{0P}}\sum_{P'\alpha'\neq P\alpha}\chi_{P'\alpha',p\alpha}\phi_{P'\alpha'}(\mathbf{r}) + \frac{\eta(\mathbf{r})}{\rho_{0P}} \quad (13)$$

$$\phi_s(\mathbf{r}) = \frac{\bar{\phi}_s}{Q_s}e^{-\omega_s(\mathbf{r})} \quad (14)$$

$$\phi_{p\alpha}(\mathbf{r}) = P_{p\alpha}(\mathbf{r})\phi_p(\mathbf{r}) \quad (15)$$

where the local volume fractions $\phi_p(\mathbf{r})$ for the triblock copolymers can be written in terms of the propagators $Q_p(\mathbf{r},t|\mathbf{r}')$ and $P_{p\alpha}(\mathbf{r})$ is the probability of a polymer segment in the internal state α, which is

$$P_{p\alpha}(\mathbf{r}) = \frac{g_{p\alpha}\exp[-\beta E_{p\alpha} - \omega_{p\alpha}(\mathbf{r})]}{\sum_\alpha g_{p\alpha}\exp[-\beta E_{p\alpha} - \omega_{p\alpha}(\mathbf{r})]} \quad (16)$$

The mean-field free energy is then obtained by inserting the mean-field solution into the free energy expression (eq 9). To obtain the solutions, mean-field equations (eqs 11−15) must be solved self-consistently using numerical methods. Unlike the approximate real-space method employed by Noolandi and coworker,[11] we use the reciprocal-space method developed by Matsen and Schick,[25] which is based on an expansion in terms of plane-wave like basis functions. This is done by reformulating these equations in the reciprocal space of a set of basis functions. All the functions with a given space-group symmetry are expanded in terms of the orthonormal basis functions as $g(\mathbf{r}) = \sum_i g_i f_i(\mathbf{r})$, where the basis functions $f_i(\mathbf{r})$ are eigenfunctions of the Laplacian operator ∇^2 with an appropriate space-group symmetry, i.e., $\nabla^2 f_i(\mathbf{r}) = -\lambda_i/D^2 f_i(\mathbf{r})$. In particular, we take $\lambda_1 = 0$ and $f_1(\mathbf{r}) = 1$. D is the period of the structure under consideration. The expansion coefficient g_i can be easily obtained by using the orthonormal relation if the function $g(\mathbf{r})$ is known

$$g_i = \int dr\, f_i(\mathbf{r})g(\mathbf{r}) \quad (17)$$

For the model with internal degrees of freedom, we will need to evaluate the expansion coefficients of some functions of $g(\mathbf{r})$, i.e., $A(r) = A(g(\mathbf{r}))$, where the function $g(\mathbf{r})$ is known, thus the expansion coefficients g_i are given. The question is how one could obtain the coefficient A_i in term of g_i from the definition,

$$A_i = \int dr\, f_i(\mathbf{r})A(g(\mathbf{r})) \quad (18)$$

In general the relationship $A(r) = A(g(\mathbf{r}))$ is not linear. For example, in this paper the effective potential $\omega_p^{\text{eff}}(\mathbf{r})$ depends on the external mean fields, $\omega_{p\alpha}(\mathbf{r})$, through eq 6. Therefore, it is not possible to obtain A_i in terms of g_i directly. It turns out that the evaluation of A_i in term of g_i can be carried out by a matrix method. Details of the formulation are found in Appendix.

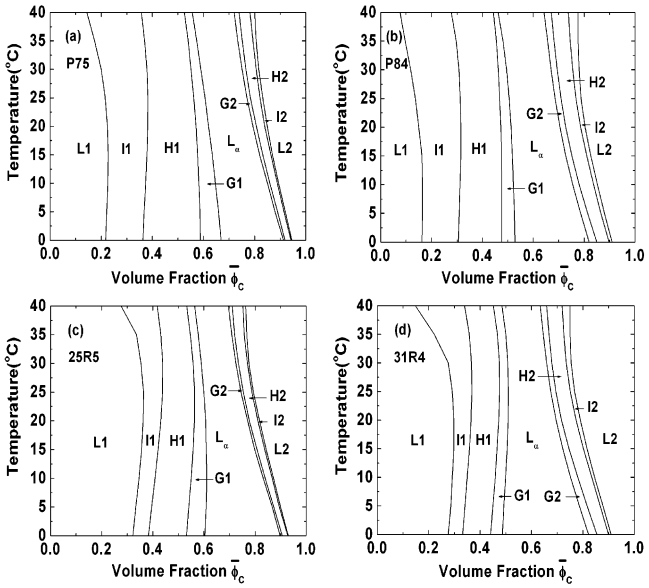

Figure 1. Calculated binary phase concentration−temperature phase diagrams for (a) Pluronic P75/water, (b) Pluronic P84/water, (c) Pluronic-R 25R5/water, and (d) Pluronic- R 31R4/water systems. L1 refers to a rich−water disordered solution, I1 the cubic phase, H1 the normal hexagonal phase, G1 the normal bicontinuous cubic phase, L_α the lamellar phase, G2 the reverse bicontinuous cubic phase, H2 the reverse hexagonal phase, I2 the reverse cubic phase, and L2 the polymer-rich disordered solution. P75, P84, 25R5, and 31R4 have almost the same molecular weight.

III. Results and Discussions

Phase Diagrams. With the reciprocal space formulation, the self-consistent field equations can be solved iteratively.[26] Having found a solution for the self-consistent field equations, the free energy is calculated. For an ordered structure the free energy has to be minimized with respect to the period *D*. Finally a phase diagram is constructed by comparing the free energies of the different structures and selecting the one with the lowest free energy as the equilibrium structure. In this paper, our main aim is to examine the approximate locations of the one-phase regions and to study their shift with composition as well as the structure of the repetitive domains. Thus, we have simplified the procedure by neglecting the two-phase regions around the phase boundaries. The two-phase regions may be obtained by using the usual double-tangent constructions.[12] In our study, seven ordered phases and one disordered phase were used for the determination of the phase diagrams. Figure 1 shows the calculated concentration−temperature phase diagrams for four triblock copolymers, $(EO)_{24}(PO)_{36}(EO)_{24}$ (P75), $(EO)_{19}(PO)_{43}(EO)_{19}$ (P84), $(PO)_{18}(EO)_{48}(PO)_{18}$ (25R5), and $(PO)_{21}(EO)_{38}(PO)_{21}$ (31R4), in aqueous solutions. All these copolymers have approximately the same average molecular weight (∼4200). The solid lines represent the phase boundary between different phases and the one-phase regions are denoted (in order of increasing polymer concentration) as L1 (water-rich disordered solution), I1 (ordered cubic phase), H1 (normal hexagonal phase), G1 (normal bicontinuous cubic phase), L_α (lamellar phase), G2 (reverse bicontinuous cubic phase), H2 (reverse hexagonal phase), I2(reverse cubic phase), and L2 (polymer-rich disordered solution).

As shown in Figure 1b, our phase diagram exhibits many similarities to the experimental results by Alexandridis et al.[9] on the phase behavior of the ternary system P84/water/*p*-xylene at 25 °C. In particular, the phases and their structure, as well as their relative location, are in good agreement with the experiments. One noticeable exception is the absence of the inversed structures (G2, H2, I2) in the experimental phase diagram along the Pluronic/water line. This discrepancy can be understood by noticing that the theoretical phase diagrams predict very narrow regions of the inversed phases (water-in-oil). Furthermore, the free energy differences between these inversed phases are very small. It is reasonable to argue that the inversed phases are not easily observed in experiments. A comparison between the phase diagrams of P75 and P84 shows that an increase in PO ratio enlarges the phase regions of the reversed phases. This is consistent with the experiments of Alexandridis and co-workers, where the addition of *p*-xylene (oil) increases the volume fraction of the nonpolar components and facilitates the formation of the inverse phases (water-in-oil). However, we notice that there are differences, such as the precise location of the boundaries, between the experimental and predicted phase diagrams. These differences could be attributed to a number of factors associated with our simple model, such as fluctuation effects, actual sizes of the monomers and sample polydispersities.

The block (EO/PO) ratio is also an important factor determining the phase behavior of the binary copolymer/water systems. For the specific case of interest here, P75 has the same EO/PO ratio (∼1.33) as 25R5, and is 48% higher than that (∼0.90) of P84 and 31R4. By comparing Figure 1a and Figure 1b for copolymers of the same molecular weight (∼4200) and chain architecture (PEO−PPO−PEO sequence), we notice that the P75/water system forms more extended normal phase regions (I1, H1, and G1) and narrower reverse phase regions (H2, G2, and I2) than those in P84/water system. A comparison between Figure 1c and Figure 1d for copolymers with the same molecular weight (∼4200) and chain architecture (PPO−PEO−PPO sequence) leads to similar conclusions. Therefore, a high EO/PO ratio favors the normal structures (oil-in-water), while a low EO/PO ratio favors the inverse structures (water-in-oil). This conclusion is consistent with earlier experimental and theoretical findings.[12]

A comparison between Figure 1a and Figure 1c (or between Figure 1b and Figure 1d) for copolymers with the same molecular weight (∼4200) and block (EO/PO) ratio (∼1.33) allows the elucidation of the effect of chain architecture on the phase behavior for the binary copolymer/water systems. In Figure 1c, the regions of the normal phases (oil-in-water) are narrower than that in Figure 1a, which indicate the normal phases are not easy to form in the reverse chain architecture (PPO−PEO−PPO sequence) systems. This conclusion has been experimentally confirmed by Alexandridis et al., who studied the phase behavior of the ternary system 25R4/water/*p*-xylene at 25 °C.[13] In this experiment, it is interesting to note that, at 25 °C, the normal hexagonal structure is not stable along the copolymer−water binary axis. However, the presence of a small amount of *p*-xylene increases the segregation of the PEO and PPO blocks and helps stabilize the hexagonal structure. This is usually explained as the entropic penalty of localizing the outer PPO blocks in the hydrophobic interior of the micelles.[27] Comparison between Figure 1b and Figure 1d for copolymers with the same molecular weight (∼4200) and block (EO/PO) ratio (∼0.90) leads to similar conclusions.

Density Profiles. The density profiles for each species (water, EO, and PO) can be obtained from the theoretical model. Since the calculation of the density profiles gives similar results for these copolymer−water systems, the density profiles are given using Pluronic P84 as an example. Figure 2 shows the density profiles for P84 at two different temperatures (15 and 40 °C) and three different morphologies (H_1, L_α, and H_2).

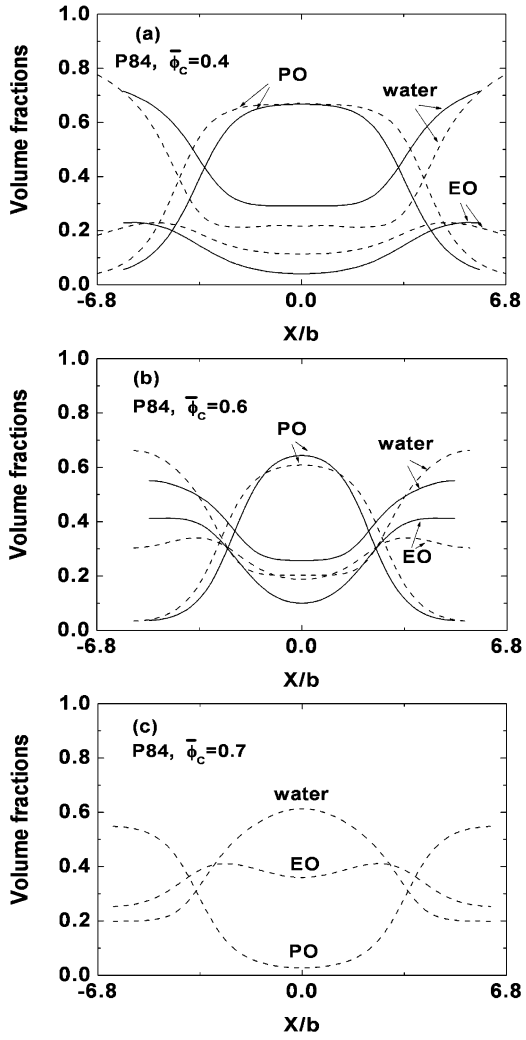

Figure 2. Calculated volume fractions profiles in the (a) normal hexagonal phase, (b) lamellar phase, and (c) reverse hexagonal phase for the P84/water system at 15 °C (full lines) and 40 °C (dash lines). The overall volume fractions $\bar{\phi}_c$ are 0.4, 0.6, and 0.7 for the normal hexagonal, lamellar, and reverse hexagonal phases, respectively.

The density profiles for the normal hexagonal phase (H1) are shown in Figure 2a for P84. At the lower temperature (15 °C), The center of the cylinder has a high concentration of PO. The EO segments are expelled from the PO domain with a tendency to stay with the water because of the hydrophilic behavior for EO at this temperature. At the higher temperature, the EO segments become more hydrophobic, it tries to withdraw into the PO domain to reduce its contact with water. However, neither water nor the PO is ideal for EO, and hence the EO volume fraction profiles display a maximum between these two regions. This can be seen more clearly in the two-dimensional density plots (Figure 3), where the EO domains show ringlike structures at the higher temperature. On the other hand, the domain spacing is increased at the higher temperature, indicating that there is a smaller interfacial area for the molecules at the higher temperature, consistent with the increased hydrophobicity of the EO and PO segments.

Figure 2b shows the density profiles for the lamellar phase (L_α). The generic features are the same as that for the hexagonal phase. In Figure 2c, the density profiles for the reverse hexagonal phase (H2) are shown. In this case, water reaches a high concentration in the interior of the cylindrical domains, whereas a high PO volume fraction is obtained outside them. Since the inverse hexagonal phase is narrow, only one temperature profile is shown.

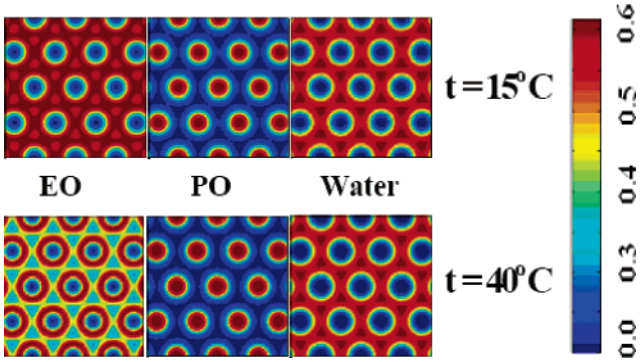

Figure 3. Two-dimensional images corresponding to the volume fractions of monomeric components for P84, hexagonal phase (H1) (shown in Figure 2a), at t = 15 °C and t = 40 °C, with an overall volume fraction of copolymer $\bar{\phi}_c$ = 0.4.

IV. Conclusions

The phase behavior of poly(ethylene oxide) (PEO) and poly(propylene oxide) (PPO) triblock copolymers in aqueous solutions is examined theoretically. The polymer−water interactions are modeled using a two-state model for the monomers. A self-consistent mean-field theory (SCMFT) is formulated for the two-state model. The reciprocal space method of SCMFT is extended to the situations where there are spatially invariant internal state energies, provided that the internal states are considered as embedded in a self-consistent potential determined by the spatial arrangement of the molecules. The method made it possible to compute the free-energy of various lyotropic liquid crystalline phases, including the complex bicontinuous gyroid phases. The method should also be useful for describing ternary triblock copolymer/water/oil phase diagrams.

The development of the self-consistent mean-field theory for polymer systems with internal degrees of freedom enabled us to make accurate free energy computations for a variety of ordered structures including the complex gyroid phase. Binary concentration−temperature phase diagrams have been constructed for a number of PEO/PPO triblock copolymers (P75, P84, 25R5, and 31R4) in aqueous solutions. The phase diagrams exhibited a number of lyotropic liquid crystalline phases: L1 (water-rich disordered solution), I1 (ordered cubic phase), H1 (normal hexagonal phase), G1 (normal bicontinuous cubic phase), L_α (lamellar phase), G2 (reverse bicontinuous cubic phase), H2 (reverse hexagonal phase), I2(reverse cubic phase), and L2 (polymer-rich disordered solution) with increasing polymer concentration. The results are consistent with available experiments and previous theoretical studies. Furthermore, systematic effects of the block (EO/PO) ratio and the chain architecture on the phase behavior for the binary copolymer/water systems have been obtained.

The density profiles for the EO, PO, and water components in the self-assembled microstructures showed the segregation between the different species became more pronounced upon heating, as a result of the decreased solubility of EO and PO in water at high temperatures. The domain spacing is increased at the higher temperature, indicating that there is a smaller interfacial area for the molecules at the higher temperature, consistent with the increased hydrophobicity of the EO and PO segments.

Appendix: Computation of Expansion Coefficients

In this appendix we present details of the computation of the expansion coefficients by a matrix approach. The matrix representation of $A(\mathbf{r}) = A(g(\mathbf{r}))$can be expressed in terms of the matrix representation of $g(\mathbf{r})$. Specifically, we define a symmetric matrix for any given function $g(\mathbf{r})$ by the relation

$$g_{ij} \equiv \int \mathrm{d}\mathbf{r}\, f_i(\mathbf{r}) f_j(\mathbf{r}) g(\mathbf{r}) = \sum_k \Gamma_{ijk} g_k \tag{A1}$$

where the tensor Γ_{ijk} is defined by $\Gamma_{ijk} \equiv V^{-1} \int f_m(\mathbf{r}) f_n(\mathbf{r}) f_i(\mathbf{r})\, \mathrm{d}\mathbf{r}$. The original expansion coefficients g_i are obtained from g_{ij} simply by $g_i = g_{1i}$ because we have chosen $f_1(\mathbf{r}) = 1$. It can be easily shown that the matrix presentation of a product of any two functions is simply the matrix product of the two matrices

$$(gh)_{ij} = \sum_k g_{ik} h_{kj} \tag{A2}$$

Using this relation it is straightforward to show that, for any function of $g(\mathbf{r})$, $A(\mathbf{r}) = A(g(\mathbf{r}))$, the matrix representation of A is simply given by the function of the matrix of g, $A = A(g)$.

This matrix relation can now be used to obtain the matrix elements A_{ij} from the matrix g. The basic idea is that, since g is a real-symmetric matrix, we can always diagonalize it to obtain the eigenvalues ϵ_n and corresponding eigenvectors υ_n such that $g \cdot \upsilon_n = \epsilon_n \upsilon_n$. Explicitly this can be written as

$$\sum_j g_{ij} \upsilon_{jn} = \epsilon_n \upsilon_{in} \tag{A3}$$

The eigenvectors $U_{ij} = \upsilon_{ij}$ are orthonormal and complete,

$$\sum_i \upsilon_{in} \upsilon_{im} = \delta_{nm}; \quad \sum_n \upsilon_{in} \upsilon_{jn} = \delta_{ij} \tag{A4}$$

The matrix formed by the element of the eigenvectors

$$U = \begin{pmatrix} v_{11} & v_{12} & \cdots & v_{1N} \\ v_{21} & v_{22} & \cdots & v_{2N} \\ \vdots & \vdots & \ddots & \vdots \\ v_{N1} & v_{N2} & \cdots & v_{NN} \end{pmatrix}; \quad U^+ = \begin{pmatrix} v_{11} & v_{21} & \cdots & v_{N1} \\ v_{12} & v_{22} & \cdots & v_{N2} \\ \vdots & \vdots & \ddots & \vdots \\ v_{1N} & v_{2N} & \cdots & v_{NN} \end{pmatrix} \tag{A5}$$

It is easy to show that U is unitary $UU^+ = U^+ U = I$. A unitary transformation by U takes the matrix g into a diagonal form

$$U^+ g U = \begin{pmatrix} \varepsilon_1 & 0 & 0 \\ 0 & \varepsilon_2 & 0 \\ 0 & 0 & \ddots \end{pmatrix} \tag{A6}$$

Therefore, for any function $A = A(g)$ we can use the identity $A = UU^+ A(g) UU^+$ to obtain

$$A_{ij} = \sum_{kl} U_{ik} A(\epsilon_k) \delta_{kl} U_{lj}^{+} \tag{A7}$$

Therefore, the matrix elements of $A = A(g)$ is given by $A_{ij} = \sum_k \upsilon_{ik} A(\epsilon_k) \upsilon_{jk}$.

In conclusion, the expansion coefficients A_i of a function $A(\mathbf{r}) = A(g(\mathbf{r}))$ can be obtained from the known coefficients g_i by the following steps:

(1) Construct a real-symmetric matrix using the relation $g_{ij} = \sum_k \Gamma_{ijk} g_k$;

(2) Diagonalize the matrix g_{ij} to obtain its eigenvalues ϵ_n and corresponding eigenvectors υ_{in}.

(3) Compute the matrix elements $A_{ij} = \sum_k A(\epsilon_k) \upsilon_{ik} \upsilon_{jk}$, the expansion coefficients are given by $A_i = A_{1i}$.

Acknowledgment. This research was supported by the National Natural Science Foundation of China (Grant Nos. 20474034, 20374031, 20373029), by the Chinese Ministry of Education with the Program of the Joint-Research Foundation of the Nankai and Tianjin Universities and the Program of New Century Excellent Talents in University, and by Nankai University ISC. A.-C.S. acknowledges the support by the Natural Science and Engineering Council (NSERC) of Canada.

References and Notes

(1) Bates, F. S.; Fredrickson, G. H. *Phys. Today.* **1999**, *52*, 32.
(2) Hamley, I. W. *Physics of block copolymers*; Oxford University Press: Oxford, England, 1998.
(3) Matsen, M. W. *J. Phys.*: *Condens. Matter* **2002**, *14*, R21.
(4) Mortensen, K. *J. Phys.*: *Condens. Matter* **1996**, *8*, A103.
(5) Marinov, G.; Michels, B.; Zana, R. *Langmuir* **1998**, *14*, 2639.
(6) Washhurn, N. R.; Lodge, T. P.; Bates, F. S. *J. Phys. Chem.* **2000**, *104*, 6987.
(7) Shusharina, N. P.; Alexandridis, P.; Linse, P.; Balijepalli, B.; Gruenbauer, H. J. M. *Eur. Phys. J. E.* **2003**, *10*, 45.
(8) Schmolka, I. R. In *Nonionic Surfactants*; Schick, M. J., Ed.; Marcel Dekker: New York, 1967; Chapter 10.
(9) Alexandridis, P.; Olsson, U.; Lindman, B. *Langmuir* **1998**, *14*, 2627.
(10) Zhang, K.; Khan, A. *Macromolecules* **1995**, *28*, 3807.
(11) Noolandi, J.; Shi, A.-C.; Linse, P. *Macromolecules* **1996**, *29*, 5907.
(12) Svensson, M.; Alexandridis, P.; Linse, P. *Macromolecules* **1999**, *32*, 637.
(13) Alexandridis, P.; Olsson, U.; Lindman, B. *J. Phys. Chem.* **1996**, *100*, 280.
(14) Errico, G. D.; Paduano, L.; Khan, A. *J. Colloid Interface Sci.* **2004**, *279*, 379.
(15) Hong, K. M.; Noolandi, J. *Macromolecules* **1981**, *14*, 727.
(16) Karlström, G. *J. Phys. Chem.* **1985**, *89*, 4962.
(17) Malmsten, M.; Linse, P.; Zhang, K.-W. *Macromolecules* **1993**, *26*, 2905.
(18) Linse, P.; Björling, M. *Macromolecules* **1991**, *24*, 6700.
(19) Sjöberg, Å.; Karlström, G. *Macromolecules* **1989**, *22*, 1325.
(20) Linse, P. *Macromolecules* **1993**, *26*, 4437.
(21) Linse, P. *J. Phys. Chem.* **1993**, *97*, 13896.
(22) Hurter, P. N.; Scheutjens, J. M. H. M.; Hatton, T. A. *Macromolecules* **1993**, *26*, 5030.
(23) Björling, M.; Linse, P.; Karlström, G. *J. Phys. Chem.* **1990**, *94*, 471.
(24) Helfand, E. *J. Chem. Phys.* **1975**, *62*, 999.
(25) Matsen, M. W.; Schick, M. *Phys. Rev. Lett.* **1994**, *72*, 2660.
(26) Laradji. M.; Shi, A.-C.; Noolandi, J.; Desai, R. *Macromolecules* **1997**, *30*, 3242.
(27) ten Brinke, G.; Hatziioannou, G. *Macromolecules* **1987**, *20*, 486.

MA060729D